Hydrazone bimetallic complex: synthesis, characterization, in silico and biological evaluation targeting breast and lung cancer cells' G-quadruplex DNA.

Mayada S. Ali[1], Dhanachandra Kuraijam[2], Sadashiva Karnik[2,3], Laila A. Jaragh-Alhadad[1, 2*]

[1] *Dept. of Chemistry, Faculty of Science, Kuwait University, Kuwait, 13060.*
[2] *Dept. of Cardiovascular and Metabolic Sciences, Cleveland Clinic Lerner Research Institute, Cleveland, Ohio 44195*
[3] *Cleveland Clinic Learner College of Medicine, Case Western Reserve University, Cleveland, Ohio, 44195*

**Corresponding author: laila.alhadad@ku.edu.kw*

Abstract

Manganese complex of (N'^1E,N'^3E)-N'^1,N'^3-bis(2-hydroxybenzylidene)isophthalo-hydrazide [H_4L] was designed, spectroscopically analyzed, and confirmed via GC-MS, FTIR, CHNS, UV-VIS, magnetic susceptibility measurements, and molar electric conductivity. The data confirmed the formation of ligand H_4L and $[Mn_2(H_2L)Cl]Cl.2H_2O$ complex. Ligand H_4L acts as a bi-negative hexadentate and tetra-negative hexadentate coordinating through two amide carbonyl, two azomethine, and two deprotonated OH groups. The magnetic and spectral data proposed a square-planar and a tetrahedral structure. The TGA data confirmed the final metal oxide form for the Mn ligand complex. Additionally, an in-vitro assessment of the ligand H_4L confirmed its ability to control cancer cell proliferation in both breast (MCF7) and lung (A549) cancer cell lines while the Mn ligand complex possessed an anticancer effect in both cancer cells at the nano-molar level. Further, the in silico data showed four hydrogen bond interactions of the ligand with G-quadruplex DNA. This strengthens our hypothesis that the hydrazone complex acts as an anticancer agent by targeting the G-quadruplex DNA.

Keywords: Biological assessment; G-quadruplex, in silico assessment; metal complex; spectroscopic analysis.

1. Introduction

Hydrazone compound and its derivatives gained a lot of attention because of their various properties such as anti-bacterial (Wu *et al*., 2018), anti-convulsant (Popiołek, 2017; Sinah *et al*., 2011), analgesic (Verma *et al*., 2014; Asif & Husain 2013; Mohareb *et al*., 2010), anti-inflammatory (Asif & Husain 2013; Sharma *et al*., 2011; Gökçe *et al*., 2009; Sastry & Rao 1989), anti-malarial (Casero *et al*., 1980; Prescott 1975), anti-microbial (Metwally *et al*., 2006; Golco *et al*., 2005; Rollas *et al*., 2002), anti-tuberculosis (Mathew *et al*., 2015; Lessigiarska *et al*., 2012; Agarwel *et al*., 2005), anti-viral (Tian *et al*., 2022; Nair *et al*., 2014; Johnson *et al*., 1982), and anticancer activities (Alotabi, 2020; Senkardes *et al*., 2020; Jing-Lin *et al*., 2014; Kumar & Narasimhan 2013; Altintop *et al*., 2012).

Cancer is the major cause of death after heart disease these days (Jaragh-Alhadad & Ali, 2022; Kumar & Narasimhan 2013) although, cancer drug delivery therapeutic strategies have greatly advanced (Jaragh-Alhadad *et al*., 2022, Jaragh-Alhadad 2021). Therefore, the development of cancer

treatments and therapeutic strategies are urgently required. One important strategy nowadays is targeting DNA structure's stability (Ghafouri-Fard *et al*., 2022; Ngoepe & Clayton 2021; Couzin-Frankel, 2013) by targeting it with complexes that combine with DNA and cleave its strands and lead to variable physiological conditions (Verma *et al*., 2014). For example, clinically cisplatin and its analogs are known to be used as metallo-anticancer drugs, and their drawback is harming the normal tissues because cisplatin is targeting the genomic DNA (Palma *et al*., 2021; Cao *et al*., 2017). The genomic DNA has a variety of structures such as strand B-DNA conformation, DNA hairpins, holiday junctions, cruciform, triplexes, or G-quadruplex (Ghafouri-Fard *et al*., 2022; Monsen & Trent 2018; Cao *et al*., 2017; Bochman *et al*., 2012; Bacolla & Wells 2004). G-quadruplex nucleic acids gained increasing interest for anticancer drug targets because of their structural features (Cao *et al*., 2017; Bugaut & Balasubramanian 2012). Its building unit is a planar G-quartet, four quinine residues pairing together through hydrogen bonds between the Watson-Crick edges and the Hogsten edge of its neighbor (Bugaut & Balasubramanian 2012). These G-quadruplex are stabilized by alkali metal cations and are located in the human chromosome's telomerase, the promoters of the oncogene, and some regions of the untranslated RNA (Cao *et al*., 2017; Bugaut & Balasubramanian , 2012; Dinshow *et al*., 2007; Burge *et al*., 2006).

Some metals when forming chemical complexes showed interesting properties such as geometric, magnetic, or catalytic (Ngoepe & Clayton, 2021) which made them ideal candidates to target the structural G-quadruplex (Cao *et al*., 2017; Jiand & Liu 2010) leading to chromosome rigidity, inhibition of DNA synthesis, and repair, and then cancer cell death (Ghafouri-Fard *et al*., 2022; Palma *et al*., 2021; Ngoepe & Clayton 2021; Cao *et al*., 2017). Further, the development of small molecules that can target G-quadruplex with alternative modes such as planar molecules (Ghafouri-Fard *et al*., 2022; Wang *et al*., 2010), loop binding molecules (Suntharalingam *et al*., 2009) electrostatic interactions (Cao *et al*., 2017) direct interactions to the nucleic acids' bases or the phosphate backbone of DNA twisted ladder, and cationic metal substituted ligand with different geometries, have more attention these days (Palma *et al*., 2021; Cao *et al*., 2017; Muller & Rodriguez 2014; Jiang & Liu, 2010; Wang *et al*., 2010; Suntharalingam *et al*., 2009). Previously, a study found that main group metals and transition metals complexes' of TMPyP4 such as Ni (II), Mn (III), Mg (II), Cu (II), Zn (II), Pd (II), Pt (II), Fe (III), and Co (II) have an electrostatic interaction with the negative DNA backbone of G-quadruplex (Cao *et al*., 2017). Furthermore, an in silico study was conducted to stabilize G-quadruplex with Pt II complexes and the data revealed high anticancer activities and especially found in the scaffolds that contain amine side chains (Wang *et al*., 2010). Another study proved the direct coordination of Pt II to the G-quadruplex DNA through a single site or cross-linking which induces the cleavage (Suntharalingam *et al*., 2009).

In 2020, Amato *et al*.,2020 used mono-hydrazone derivatives to target G-quadruplex structures and increase the R-loop in human cancer cells. The data proved mono hydrazones' ability to kill cancer cells and their potent effect on genome instability (Amato *et al*., 2020). Previously, several series of hydrazone anticancer compounds were synthesized, well-characterized, and proved to be anticancer agents (El-Asmy *et al*., 2016 , 2015). Based on that, in the present research hydrazone derivative (N'1E,N'3E)-N'1,N'3-bis(2-hydroxybenzylidene)-isophthalohydrazide [H_4L] ligand and its Mn ligand complex were designed, synthesized, and spectroscopically characterized. In addition, the in silico study for the ligand to prove the interactions with G-quadruplex DNA. Also, biological evaluation for both ligand and Mn ligand complex against breast (MCF7) and lung (A549) cancers as surrogate in-vitro models.

2. Experimental

2.1. Materials and methods

Chemicals such as $MnCl_2.2H_2O$, isophthalic dihydrazone, 2-hydroxy-benzaldehyde, absolute ethanol, diethyl ether, and DMSO were obtained from the BDH Chemicals. The physical measurements: Varian Micro V1.5.8, CHNS Mode, 15073036 was used for elemental analysis of HBIH and its complexes at the Microanalytical Unit. The metal content was determined using ICP-OES GBC Quantum Sequential. FTIR spectra were recorded as KBr discs on an FT/IR-6300 type A (400-4000 cm^{-1}). Electronic spectra of the complexes were recorded on Cary 5 UV-VIS Spectrophotometer, Varian (200-900 nm). Molecular weights were recorded on a GC-MS Thermo-DFS (BG_FAB) mass spectrometer. Samples' magnetic susceptibility was measured using a Johnson-Matthey magnetic balance, UK. $Hg[Co(SCN)_4]$ was used as a calibrant for diamagnetism which was calculated from Pascal's constants. All physical and chemical experiments were done at Kuwait University laboratories (RSPU).

2.2. Synthesis and analysis

2.2.1. Synthesis of (N'1E,N'3E)-N'1,N'3-bis(2-hydroxybenzylidene)isophthalo-hydrazide ligand H_4L

The ligand was prepared by adding 9.7 g (0.05 mol) of isophthalic acid dihydrazone, dissolved in 30 mL ethanol, with 12.2 g (0.1 mol) of 2-hydroxybenzaldehyde. The mixture was refluxed on a mantel for two hours. The white precipitate was filtered, recrystallized from absolute ethanol, and left to dry in a silica gel desiccator overnight. The product yield is 85% and the ligand melting point is 265-267^oC (Scheme 1).

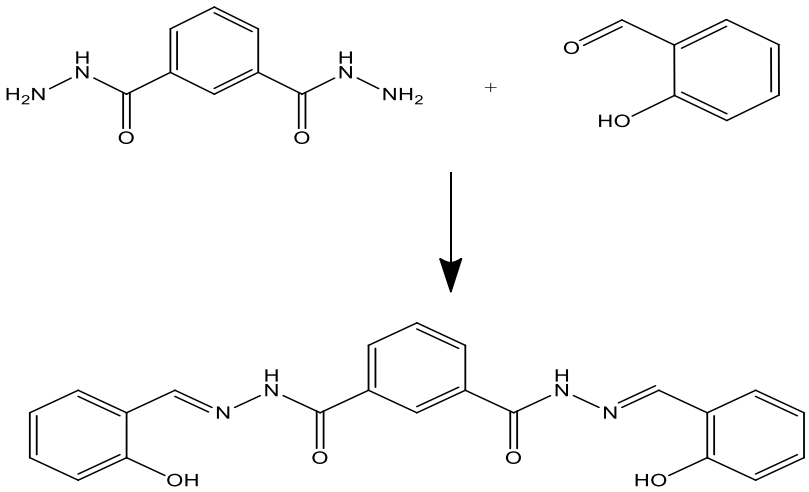

Scheme1: Synthesis of (N'1E,N'3E)-N'1,N'3-bis(2-hydroxybenzylidene)isophthalo-hydrazide ligand (H_4L).

2.2.2. Synthesis of Mn ligand complex

The metal complex was prepared by reacting the metal salt with the ligand H_4L in absolute ethanol with a ratio (2M:1L). The mixture was heated under reflux on a heating mantel and with continuous stirring for three to six hours (Figure. 1). The color of the reaction mixture directly changed and formed a colored precipitate which was filtered, washed, and dried overnight. The purity of the

compounds was formulated and established by microanalysis (El-Asmy *et al*., 2016a, El-Asmy *et al.,*2016b and El-Asmy *et al*.,2015).

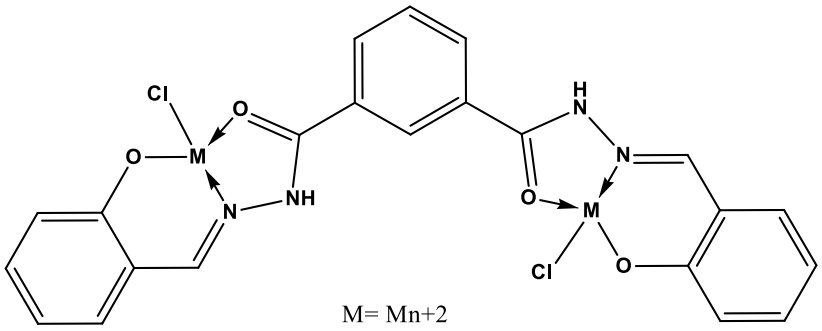

Fig. 1. The proposed structures of the Mn ligand complex.

2.3. Cell culture and cytotoxicity assay

Cell culture media, FBS, PBS, Trypsin, L-Glutathione, penicillin-streptomycin, and MCF7 cells were obtained from the media-core facility at Lerner Research Institute and used directly unless otherwise described. A549 lung cancer cells plate was a gift from Dr. Robert Silverman Laboratory in Lerner Research Institute-Cleveland Clinic. Cells were maintained in DMEM media which is supplemented with 10% FBS (activated in a water bath before use), 1% penicillin/streptomycin, and 1% L-Glutathione and kept in a 5% CO_2 incubator. Cytotoxicity assay was done based on the manufacturer's protocol provided by WST-1 assay Kit (ab65473 Abcam, USA). All experiments were done in triplicate, and the absorbance was recorded at 440 nm (Jaragh-Alhadad *et al*., 2022; Jaragh-Alhadad & Ali 2022, Jaragh-Alhadad 2018).

In-depth, five to ten thousand cells in 100 µl growth media were seeded in the wells of 96 well-plates. After 24 hr. 100 µl of various concentrations of ligand and Mn ligand complex were added to the cells and incubated for 48 hr. in a CO_2 incubator. Ten µl WST-1 reagent was added and incubated for two hrs. Followed by absorbance measurement at 440 nm by plate reader. The statistical data were analyzed in GraphPad prism software and normalized to controls by nonlinear regression analysis.

2.4. In silico molecular modeling

All the ligands were drawn in Maestro (Schrodinger, LLC, New York, NY, USA). Each structure was assigned an appropriate bond order using the LigPrep package from Schrodinger, LLC, NY, USA (Glide 2017; LigPrep 2017). The ligands were converted to Maestro format, Schrodinger, LLC, NY, USA, and geometrically optimize the ligand and computed partial atomic charges (Ngoepe & Clayton 2021). Then, at most, 32 poses per ligand were generated with different steric features for the subsequent docking study. Structure of G-quadruplexes (PDB id:2N60) with (4n-1) guanines in the G-tetrad core download from PDB (www.rcsb.org). The structure was ready and uploaded to the protein preparation wizard of Schrodinger, LLC. This was followed by, induced fit docking (IFD) (Schrodinger, LLC, NY, USA), which was used to dock all the ligands with G-quadruplex (Singh *et al*., 2018; Glide 2017; LigPrep 2017; Harder *et al*., 2016).

3. Results and discussion

3.1. Chemistry

In the present study, ligand H_4L and Mn ligand complex was designed, synthesized, physically, and chemically characterized. Ligand H_4L CHNS results coincide with the formula of HBIH. The physical data of the ligand and its metal complex such as colors, melting points, and elemental analyses are summarized in (Table 1). The data confirmed the formation of both ligand H_4L and $[Mn_2(H_2L)(H_2O)Cl]Cl.H_2O$ complex. Additionally, ligand H_4L and its metal complex are chemically characterized via GC-MS (Table 1), FTIR (Table 2), UV-VIS, magnetic susceptibility measurements, molar electric conductivity (Table 3), and TGA analysis (Table 4).

Table 1. Molecular weights, colors, melting points, and elemental analysis of H_4L and its metal complex.

Analysis	H_4L $C_{22}H_{18}N_4O_4$	$[Mn_2(H_2L)Cl]Cl.H_2O$ $C_{22}H_{20}N_4O_6Mn_2Cl_2$
M.W. (Found, m/e)	402.13 (403.6)	616.94 (595.3)
Color	White	Yellow
Λ_m	3.96	83.94
M.P., (°C)	265-267	> 320
C % Calcd. (Found)	65.71 (65.78)	42.83 (42.88)
H % Calcd. (Found)	4.51 (4.64)	3.27 (3.67)
N % Calcd. (Found)	13.93 (12.99)	9.08 (8.45)

H_4L: ligand, $[Mn_2(H_2L)Cl]Cl.H_2O$: metal-ligand complex. Λ_m is molar conductivity in Ω^{-1} cm^2 mol^{-1}

3.2. FTIR spectra analysis of ligand H_4L and its metal complex

FTIR bands are reported in (Table 2). The ligand H_4L can coordinate with metal ions because its main site is rich in chemical functional groups. Ligand's FTIR spectrum showed a band at 3244 cm^{-1} due to the overlap between ν(OH) and ν(NH), bands at 1644 and 1607 cm^{-1} which is due to ν(C=O) and ν(C=N), respectively (Golco *et al*., 2005). Mn ligand complex bands were compared with the ligand H_4L bands. The ligand H_4L acts as a mono-negative tridentate with $[Mn_2(H_2L)Cl_2].2H_2O$ complex. The new band at 1529-1547 cm^{-1} is related to the azomethine group enolization of NHC=O. The complexes' spectra showed new bands in the ranges of 520-543, and 458-558 cm^{-1} which are due to ν(M-O), ν(M-N) [18]; and ν(M-O) is observed at a higher wavenumber than ν(M-N). Also, the new band at 3338-3465 cm^{-1} is duo to ν(OH) of the coordinated water (Agarwel *et al*., 2005).

Table 2. FTIR spectral data of ligand H_4L and its metal complex.

Compound	ν(OH)	ν(N-H)	ν(C=O)	ν(C=N)	ν(C=N)*	ν(C-O)	υ(M-O)	υ(M-N)	υ(H_2O)
H_4L	3244s	3244m	1644s	1607m	-	1253w	-	-	
$[Mn_2(H_2L)Cl_2].2H_2O$	-	3233m	1619s	1574m	1547s		524m	458m	3370br

* New azomethine group due to enolization of NHC=O

3.3. Electronic and magnetic analysis

The magnetic moment values of the ligand H_4L showed that it acts as a mono-negative tridentate with Mn ligand complex, which was measured in DMSO and was between 200 to 1000 nm at room temperature, data are presented in (Table 3). The absorption spectrum of ligand H_4L in DMSO showed the $\pi \rightarrow \pi^*$ and $n \rightarrow \pi^*$ bands of C=C, C=O, and C=N groups at 34480; 33220, and 30030 cm^{-1} (Figures. 2 & 3). The electronic spectra of the Mn (II) complex displayed a new band in the visible region at 411 nm (24330 cm^{-1}) which attributed to the electronic transition $^6A_1 \rightarrow {}^4T_{1(G)}$. Thus, the magnetic moment value is 3.52 B.M, demonstrating that the Mn (II) complex is paramagnetic and has high spin tetrahedral geometry (Figure. 2 & 3).

Table 3. Magnetic moments and electronic spectral bands of the metal complexes.

Compound	μ_{eff} (BM)	Intra ligand and charge transfer, cm^{-1} (ε*)	d-d transition (cm^{-1})	Proposed structure
H_4L	---	34480 (1079); 33220 (1096); 30030 (1147)		----
$[Mn_2(H_2L)Cl_2].2H_2O$	2.52	34480 (1879); 33220 (1937)	30210 (1967) 24330 (427)	Tetrahedral

*Value for molar extension coefficient.

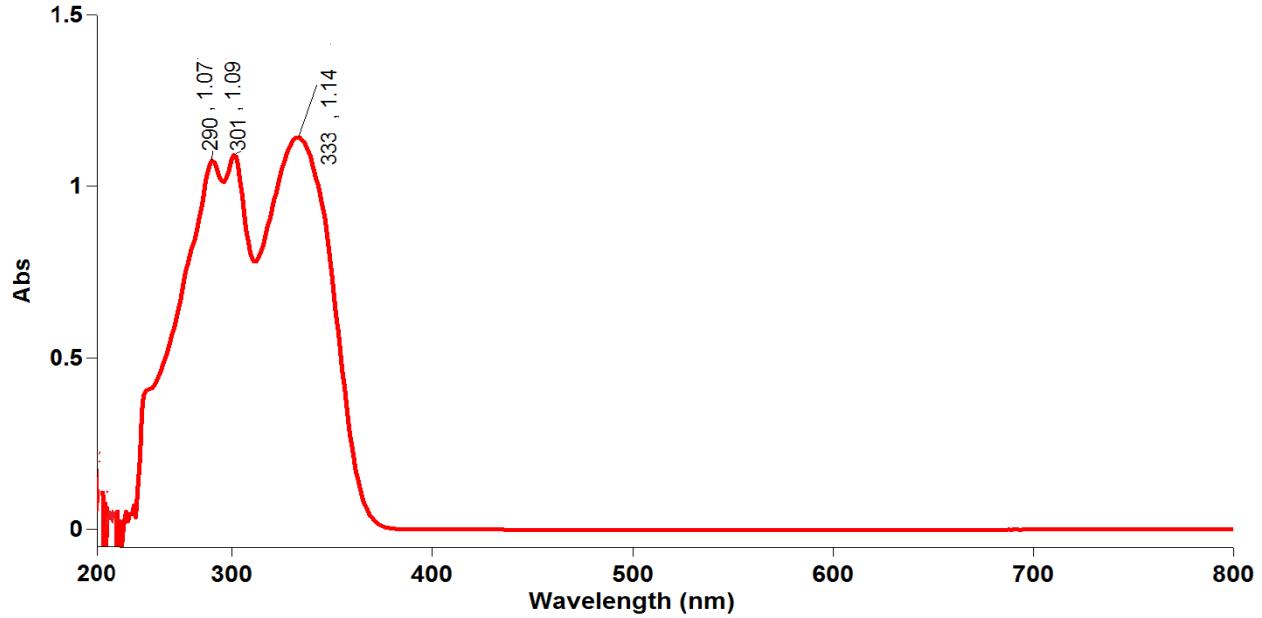

Fig. 2. Electronic spectrum of ligand H_4L.

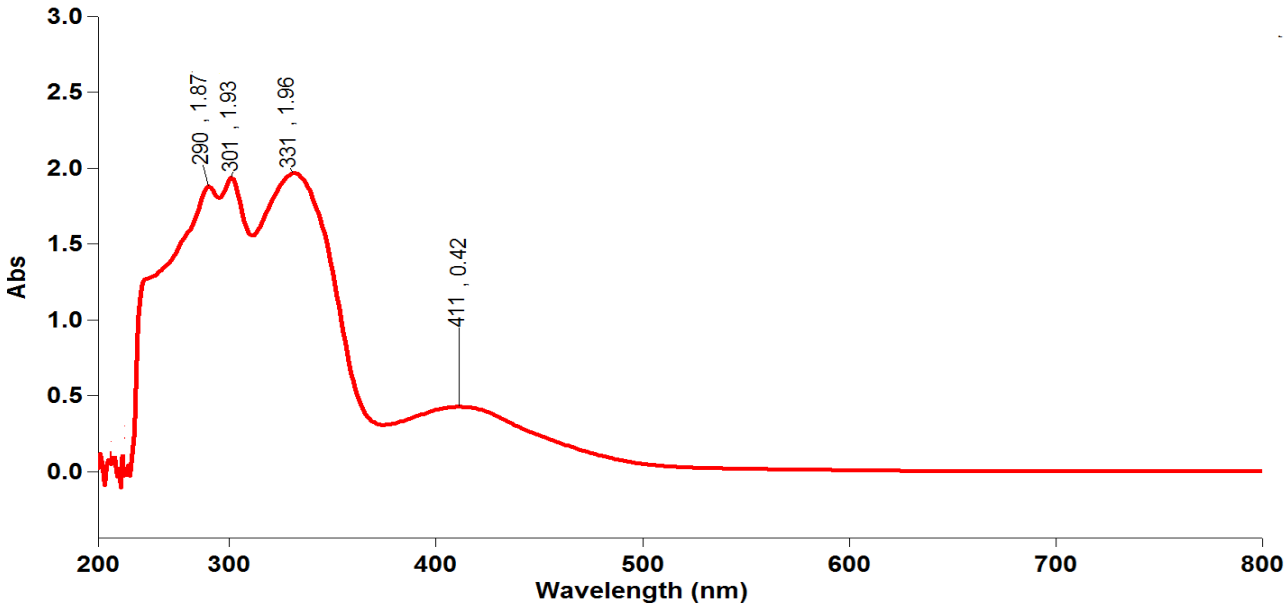

Fig. 3. Electronic spectrum of $[Mn_2(H_2L)Cl_2].2H_2O$.

3.4. Thermal Gravimetric Analysis (TGA)

The thermo-gravimetric analysis was measured in the 25 to 800 °C range (Figures. 4 & 5). The data of thermo-gravimetric are listed in (Table 4) and proved that there is an obvious the losing weight between the suggested and calculated formulae. The thermogravimetric curve of the Ligand (H_4L) verified that the ligand is thermally stable up to 190 °C. Thermal decomposition of this ligand occurred in three stages in temperature ranges: (199–222°C), (248–280 °C), and (510–800 °C). The first degradation stage showed weight loss equal to 38.15(38.55%), due to the elimination of ($C_{10}H_5NO$). However, the second degradation stage showed weight loss equal to 36.35(35.35%), attributable to the elimination of ($C_{10}H_8N$). However, the third degradation stage showed weight loss

equal to 23.31(26.12%), referring to complete pyrolysis of the Hydrazone. The thermogram curve of the Mn II complex verified that the complex is thermally stable up to 300 °C. The thermal decomposition of this complex occurred in one stage in the temperature range: (305–750 °C) with weight loss equal to 74.59(77.04%), which is attributed to complete pyrolysis of the complex, leaving 2MnO as a residue.

Table 4. Thermogravimetric data of H_4L and its metal complex.

compound	Temp. (°C)	Weight loss (%) Found (calcd.)	assignment
H_4L **$C_{22}H_{18}N_4O_4$**	30-190	--	Stable
	199-222	38.15(38.55)	Elimination of $C_{10}H_5NO$
	248-280	36.35(35.35)	Elimination of $C_{10}H_8N$
	510-800	23.31(26.12)	Elimination of $C_2H_5N_2O_3$
$[Mn_2(H_2L)Cl]Cl.H_2O$ **$C_{22}H_{20}N_4O_6Mn_2Cl_2$**	30-300	--	Stable
	305-750	74.59(77.04)	decomposition of the complex
	800	25.40(22.99)	2MnO (residue)

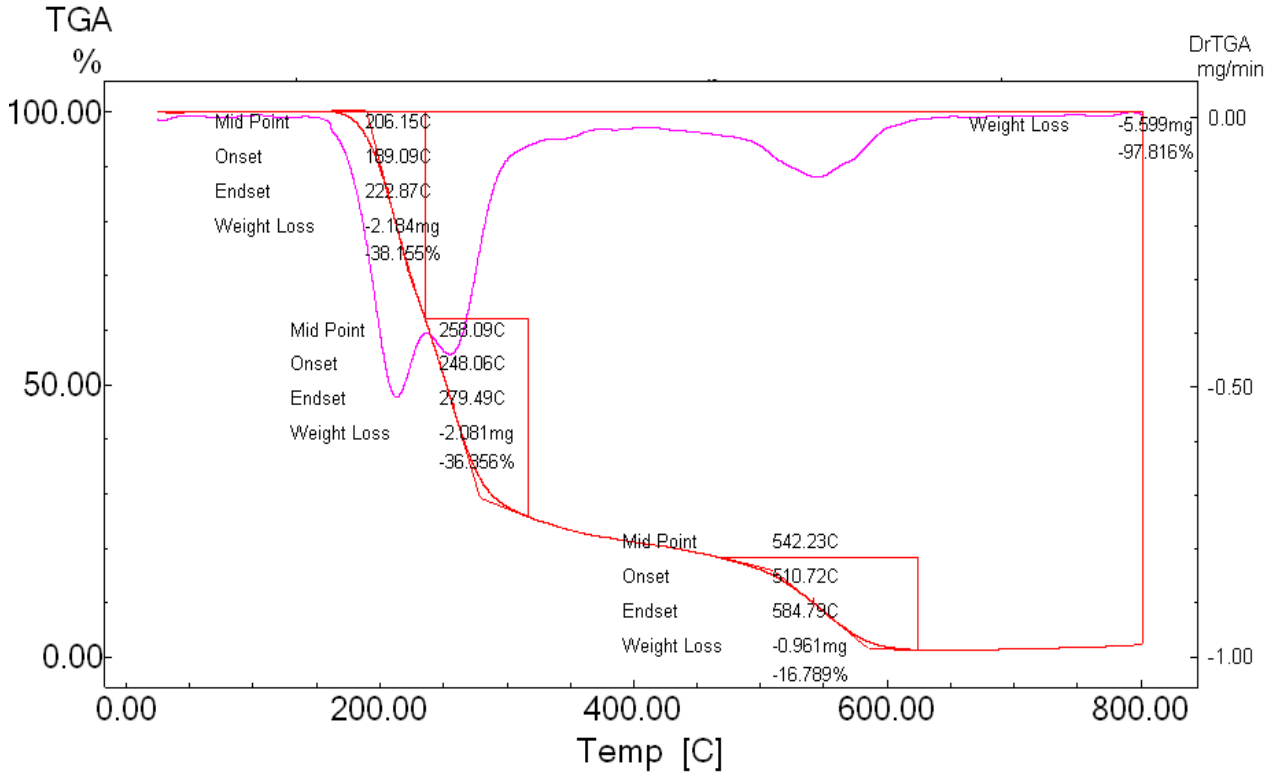

Fig. 4. The TG thermogram of the H_4L ligand.

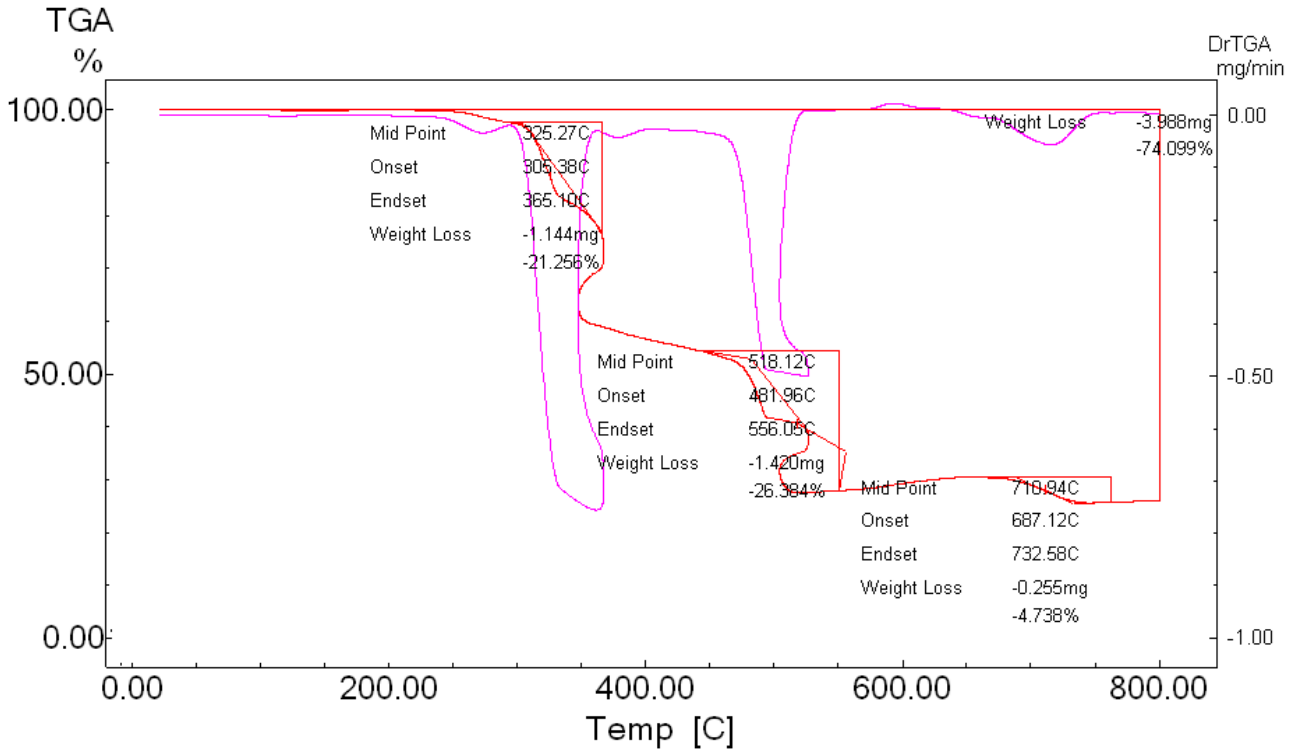

Fig. 5. The TG thermogram of Mn II complex.

3.5. Cytotoxicity assay

To further study the effect of the Mn ligand complex cytotoxicity, an MTT assay was performed using breast and lung epithelial cancer cells. MCF7 and A549 cell lines were treated with one micro-molar of the ligand H_4L, and the results showed cell growth control. While the treatment with Mn ligand complex showed potent cell growth inhibition at the same concentration. Mn ligand complex showed inhibitory activity with MCF7 and A549 cell lines reaching 168 nM, and 275 nM, respectively. The data revealed that the Mn ligand complex with tetrahedral geometry has strong biological activity through the four hydrogen bonds. Previously, it was proven that the metal center of a complex plays an essential role in metal-ligand G-quadruplex interactions, binding affinity, specificity, and telomerase inhibiting activity (Cao *et al*., 2017). Moreover, a study stated that small compound modifications such as a ligand or central metal can obtain compounds with different geometries and different biological activities (Suntharalingam *et al*., 2009; Klekota & Roth, 2008) (Table 5).

Table 5. Cancer cells are treated with the ligand and Mn-H_4L complex.

Cell line	H_4L		$[Mn_2(H_2L)Cl]Cl.2H_2O$
MCF7 breast cancer	Control cell growth	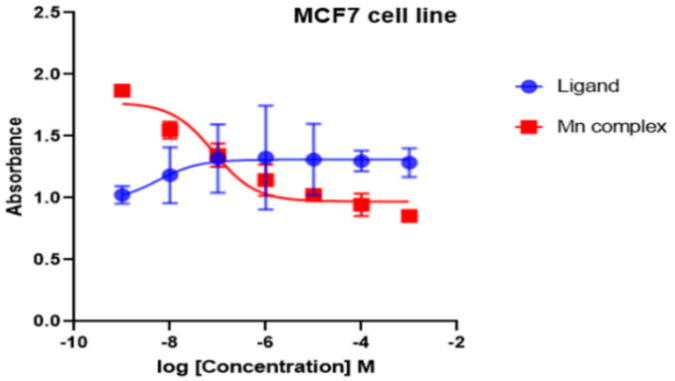	168±31.9*
A549 lung cancer	Control cell growth	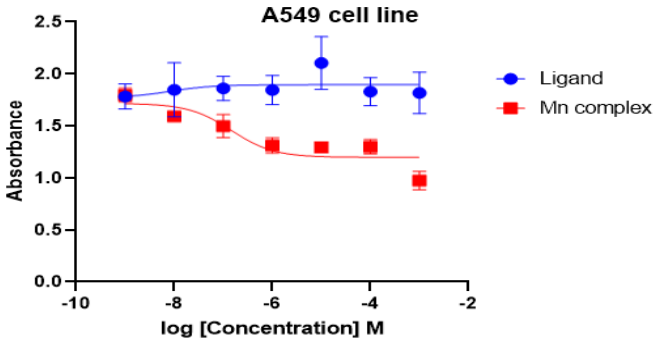	275±25.7*

The results are an average of three tests with seven dilutions and eight replicates each. The data were represented as Mean ± SD, (*P<0.0005).

3.5. In silico modeling of ligand H_4L with G-quadruplex

This test was performed to understand the insight binding activity of the ligand H_4L with G-quadruplex DNA. Structural refinement was performed and the active site with the four hydrogen bonds was predicted, and the docking score of the ligand H_4L is -5.146 kcal/mol, as shown in Figure. 6. Ligand H_4L showed potent interaction with G-quadruplex similar to 360A iodide, which is known as a selective stabilizer of the G-Quadruplex, and also showed telomerase activity inhibition which reached an IC_{50} of 300 nM for telomerase in TRAP-G4 assay and its docking score is -5.551 kcal/mol and with only one hydrogen bond (Figure. 7) (https://www.medchemexpress.com/Targets/G-quadruplex.html). The superimposition of the docked pose of 360A iodide and ligand H_4L with G-Quadruplex is shown in Figure. 8.

Research studies benefit from in silico modeling and the G-quadruplex studies and showed significant improvement in the survival rates in melanoma skin cancer patients through the development of targeted therapies and immunotherapeutic approaches (Ghafouri-Fard *et al*., 2022). In addition, a study in leukemia revealed that after G-quadruplex stabilization, the expression of oncogene and the function of the telomerase led to apoptosis in leukemia patients (Ghafouri-Fard *et al*., 2022).

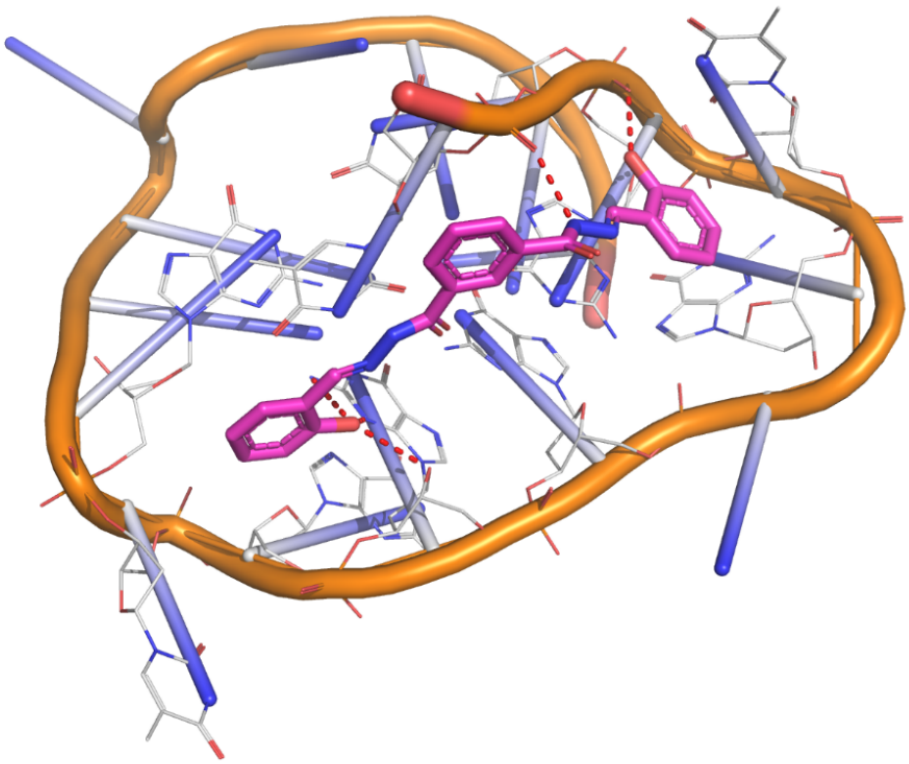

Fig. 6. Binding interactions between ligand H_4L and the G-quadruplex with four hydrogen bonds.

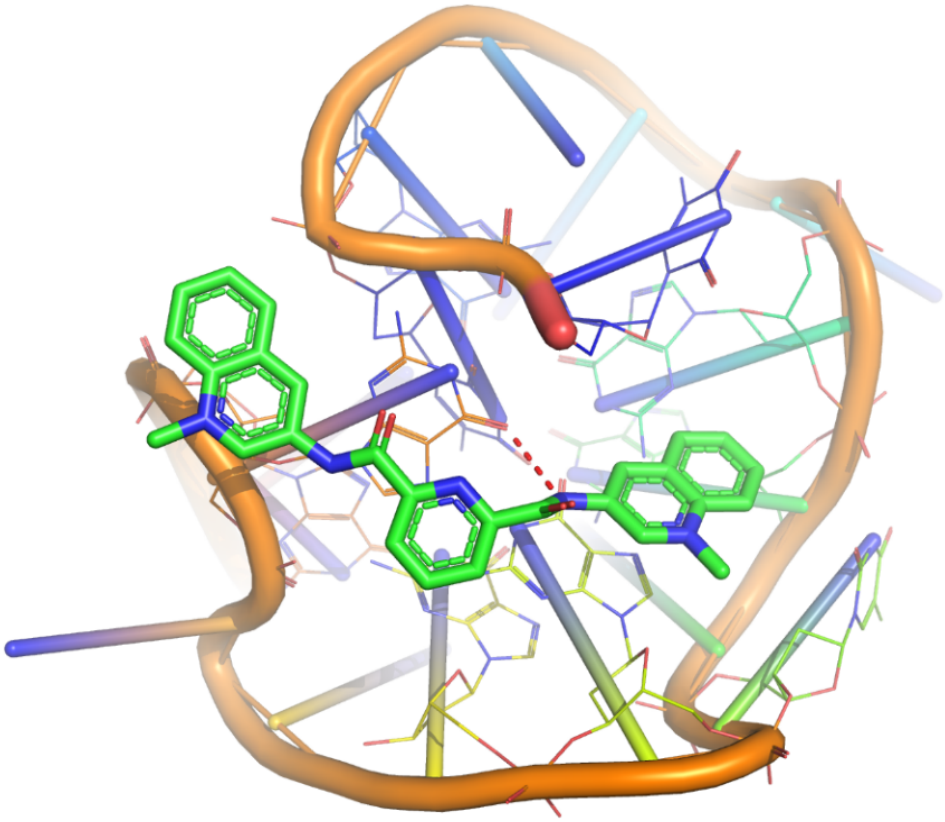

Fig. 7. Binding interactions between ligand 360A iodide and the G-quadruplex with one hydrogen bond.

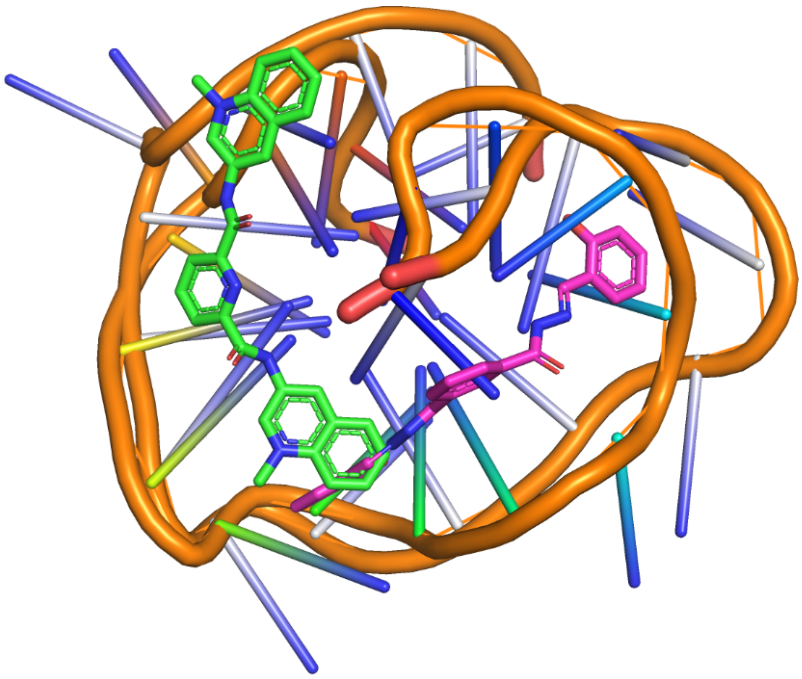

Fig. 8. Superimpose binding interactions between both ligand 360A (left) iodide and ligand H_4L (right) within the G-quadruplex.

4. Conclusion

The formation of a metal-ligand complex to target G-quadruplex structural stability has been recognized as a potential therapeutic tool for cancer drug development. The new ligand, (N'^1E, N'^3E)-N'^1,N'^3-bis(2-hydroxybenzylidene)isophthalo-hydrazide [H_4L], has been prepared and introduced for chelation with Mn II metal ion. The Mn ligand complex is spectroscopically characterized, and it is a mono-negative tridentate tetrahedral geometry. In addition, cell cytotoxicity assay results indicated that the ligand H_4L controls cancer cell growth while Mn ligand complex reduced it in both cancer cell lines at the nano-molar levels. In sum, the IC_{50} data revealed that the Mn ligand complex with tetrahedral geometry enhanced the biological activity. In addition, the insilco study supports the ligand and its interactions with G-quadruplex DNA. This study may serve as a rational design for ligand and metal complexes for drug design that targets the G-quadruplex.

Declaration of competing interest

The authors declare that they have no known competing financial interests or personal relationships that could have appeared to influence the work reported in this paper.

ACKNOWLEDGEMENTS

We are grateful for the financial support from Kuwait University grant no. (SC14/18). The authors would like to acknowledge RSPU at Kuwait University projects (GS 01/01; GS 01/03; GS 01/05; GS 03/08). In addition, the authors would like to acknowledge Lerner Research Institute- Cleveland Clinic for providing the facilities to conduct the biological tests.

References

Agarwel, R. K., Sharma, D. K., Singh, R. (2005). Synthesis, Spectral and Thermal Investigations of Some Oxovanadium(IV) Complexes of Hydrazones of Isonicotinic Acid Hydrazide, Turk J Chem, 29 (3):309-316. https://journals.tubitak.gov.tr/chem/vol29/iss3/10.

Alotabi, S. H. (2020). Synthesis, characterization, anticancer activity, and molecular docking of some new sugar hydrazone and arylidene derivatives, Arabian Journal of Chemistry, 13 (3):4771-4784. https://doi.org/10.1016/j.arabjc.2019.12.006.

Altıntop, M. D., Özdemir, A., Turan-Zitouni, G, *et al*. (2012). Synthesis and biological evaluation of some hydrazone derivatives as new anticandidal and anticancer agents, European Journal of Medicinal Chemistry, 58:299-307. https://doi.org/10.1016/j.ejmech.2012.10.011.

Amato, J., Miglietta, G., Morigi, R. Iaccarino, N., Locatelli, A., Leoni, A., Novellino, E., Pagano, P *et al*., (2020). Monohydrazone Based G-Quadruplex Selective Ligands Induce DNA Damage and Genome Instability in Human Cancer Cells, J Med Chem, 63 (6):3090-3103. https://doi.org/10.1021/acs.jmedchem.9b01866.

Asif, M., Husain, A. (2013). Analgesic, Anti-Inflammatory, and Antiplatelet Profile of Hydrazones Containing Synthetic Molecules, Journal of Applied Chemistry, 2013:ID 247203. https://doi.org/10.1155/2013/247203.

Bacolla, A., Wells, R. D. (2004). Non-B DNA conformations, genomic rearrangements, and human disease, J Biol Chem, 279 (46):47411-47414. https://doi.org/10.1074/jbc.R400028200.

Bochman, M. L, Paeschke, K., Zakian, V. A. (2012). DNA secondary structures: stability and function of G-quadruplex structures, Nat Rev Genet, 13 (11):770-780. https://doi.org/10.1038/nrg3296.

Bugaut, A., Balasubramanian, S. (2012). 5'-UTR RNA G-quadruplexes: translation regulation and targeting, Nucleic Acids Res, 40 (11):4727-4741. https://doi.org/10.1093/nar/gks068.

Burge, S., Parkinson, G. N., Hazel, P., Todd, A. K., Neidle, S. (2006). Quadruplex DNA: sequence, topology and structure, Nucleic Acids Res, 34 (19):5402-5415. https://doi.org/10.1093/nar/gkl655.

Cao, Q., Li, Y., Freisinger, E., Qin, P. Z., Sigel, R. K. O., Mao, Z.-W. (2017). G-quadruplex DNA targeted metal complexes acting as potential anticancer drugs, Inorg. Chem. Front, 4:10-32. https://doi.org/10.1039/C6QI00300A.

Casero, R. A. Jr., Klayman, D. L., Childs, G. E., Scovill, J. P., Desjardins, R. E. (1980). The activity of 2-acetylpyridine thiosemicarbazones against trypanosoma rhodesiense in vitro, Antimicrob Agents Chemother, (2) :317-22. https://doi.org/10.1128/AAC.18.2.317.

Couzin-Frankel, J. (2013). Cancer immunotherapy, Science, 342:1432-1433. https://doi.org/10.1126/science.342.6165.1432.

Dinshaw, J. P., Anh, T. P., Vitaly, K. (2007). Human telomere, oncogenic promoter and 5′-UTR G-quadruplexes: diverse higher order DNA and RNA targets for cancer therapeutics, Nucleic Acids Research, 35 (22):7429–7455. https://doi.org/10.1093/nar/gkm711.

El-Asmy, A., Jeragh, B., Ali, M. (2015). Spectral, thermal, molecular modeling and biological studies on mono- and binuclear complexes derived from oxalo bis(2,3-butanedionehydrazone), Chem Cent J, 9:69. https://doi.org/10.1186/s13065-015-0135-y.

El-Asmy, A., Jeragh, b., Ali, M. (2016a). Synthesis and characterization of tri- and tetra-metallic complexes of N'1,N'4-bis((E)-3,4-dihydroxybenzylidene)-succinohydrazide, European Journal of Chemistry, 7:81-90. https://doi.org/10.5155/eurjchem.7.1.81-90.1356.

El-Asmi, A, Jeragh, B., Ali, M. S. (2016b). Chelation activity of N'1,N'6-bis((E)-3,4-dihydroxybenzylidene)adipohydrazide towards some transition metal ions, European Journal of Chemistry, 7 (3)283-289. https://doi.org/10.5155/eurjchem.7.3.283-289.1461.

Ghafouri-Fard, S., Abak, A., Baniahmad, A., Hussen, B. M., Taheri, M., Jamali, E., Dinger, M. E. (2022). Interaction between non-coding RNAs, mRNAs and G-quadruplexes, Cancer Cell Int, 22 (1):171. https://doi.org/10.1186/s12935-022-02601-2.

Glide. (2017). Schrödinger Release 2017-2, Schrödinger, LLC: New York, NY, 2017.

Gökçe, M., Utku, S., Küpeli, E. (2009). Synthesis and analgesic and anti-inflammatory activities 6-substituted-3(2H)-pyridazinone-2-acetyl-2-(p-substituted/nonsubstituted benzal)hydrazone derivatives, Eur J Med Chem, (9) :3760-4. https://doi: 10.1016/j.ejmech.2009.04.048.

Golcu, A., Tumer, M., Demirelli, H., Wheatley, R. A. (2005). Cd(II) and Cu(II) complexes of polydentate Schiff base ligands: synthesis, characterization, properties and biological activity, Inorganica Chimica Acta, 358 (6):1785-1797. https://doi.org/10.1016/j.ica.2004.11.026.

Harder, E., Damm, W., Maple, J., *et al*. (2016). OPLS3: A Force Field Providing Broad Coverage of Drug-like Small Molecules and Proteins, J Chem Theory Comput, 12 (1):281-296. https://doi.org/10.1021/acs.jctc.5b00864.

Jaragh-Alhadad, L. (2018). In-vitro evaluation of HSP27 inhibitors function through HER2 pathway for ovarian cancer therapy, Translational Cancer Research, 7 (6):1510-1517. https://dx.doi.org/10.21037/tcr.

Jaragh-Alhadad L. A. (2021). Encapsulation and In Vitro Evaluation of Low-Density Lipoprotein with Cholesterol Conjugated Anti-HSP27 and HER2 Proteins as Drug Delivery Enhancement in Ovarian Cancer, Biomedical Journal of Scientific and Technical Research, 35 (2):27497-27504. https://doi.org/10.26717/BJSTR.2021.35.005675.

Jaragh-Alhadad, L., Ali, M. S. (2022). Nimesulide derivatives reduced cell proliferation against breast and ovarian cancer: synthesis, characterization, biological assessment, and crystal structure, Kuwait Journal of Science, 49 (3):1-17. https://doi.org/10.48129/kjs.16735.

Jaragh-Alhadad, L. A., Ali, M. S. (2022). Methoxybenzamide derivative of nimesulide from anti-fever to anti-cancer: Chemical characterization and cytotoxicity, Saudi Pharm J, 30 (5):485-493. https//doi.org/10.1016/j.jsps.2022.03.004.

Jaragh-Alhadad, L. A., Ali, M. S., Moustafa, M. S., Harisa, G. I., Alanazi, F. k., Karnik, S. (2022). Sulfonamide derivatives mediate breast and lung cancer cell line killing through tubulin inhibition, Journal of Molecular Structure, 1268(133699). https://doi.org/10.1016/j.molstruc.2022.133699.

Jaragh-Alhadad , L., Samir , M., Harford, T. J., Karnik, S. (2022). Low-density lipoprotein encapsulated thiosemicarbazone metal complexes is active targeting vehicle for breast, lung, and prostate cancers, Drug delivery, 29 (1):2206- 2216. https://doi.org/10.1080/10717544.2022.2096713.

Jiang, Y. L., Liu, Z. P. (2010). Metallo-organic G-quadruplex ligands in anticancer drug design, Mini Rev Med Chem, 10 (8):726-736. https://doi.org/10.2174/138955710791572433.

Jing-lin, W., Ya-qin, Z., Bin-sheng, Y. (2014). Transition metal complexes of asymmetrical aroyl-hydrazone ligand: Syntheses, structures, DNA binding and cleavage studies, Inorganica Chimica Acta: B, 409:484-496. https://doi.org/10.1016/j.ica.2013.09.001.

Johnson, D. K., Murphy, T. b., Rose, N. J., Goodwin, W. H., Pickart, L. (1982). Cytotoxic chelators and chelates 1. Inhibition of DNA synthesis in cultured rodent and human cells by aroylhydrazones and by a copper(II) complex of salicylaldehyde benzoyl hydrazone, Inorganica Chimica Acta, 67:159-165. https://doi.org/10.1016/S0020-1693(00)85058-6.

Klekota, J., Roth, F. P. (2008). Chemical substructures that enrich for biological activity, Bioinformatics, 24 (21):2518-2525. https://doi.org/10.1093/bioinformatics/btn479.

Kumar, P., Narasimhan, B. (2013). Hydrazides/hydrazones as antimicrobial and anticancer agents in the new millennium, Mini Rev Med Chem, 13 (7):971-987. https://doi.org/10.2174/1389557511313070003.

LigPrep. (2017). Schrödinger Release 2017-2, Schrödinger, LLC: New York, NY, 2017.

Lessigiarska, I., Pajeva, I., Prodanova, P., Georgieva, M., Bijev, A. (2012). Structure-activity relationships of pyrrole hydrazones as new anti-tuberculosis agents, Med Chem, 8 (3):462-473. https://doi.org/10.2174/1573406411208030462.

Mathew, B., Suresh, J., Ahsan, M. J, *et al*. (2015). Hydrazones as a privileged structural linker in antitubercular agents: a review, Infectious Disorders Drug Targets, 15 (2):76-88. https://doi.org/10.2174/1871526515666150724104411.

Metwally, K. A., Abdel-Aziz, L. M., Lashine, el-SM., Husseiny, M. I., Badawy, R. H. (2006). Hydrazones of 2-aryl-quinoline-4-carboxylic acid hydrazides: synthesis and preliminary evaluation as antimicrobial agents, Bioorg Med Chem, (24):8675-8682. https://doi.org/10.1016/j.bmc.2006.08.022.

Muller, S., Rodriguez, R. (2014). G-quadruplex interacting small molecules and drugs: from bench toward bedside, Expert Review of Clinical Pharmacology, 7 (5):1751-2433. https://doi.org/10.1586/17512433.2014.945909.

Mohareb, R. M., El-Sharkawy, K. A., Hussein, M. M., El-Sehrawi, H. M. (2010). Synthesis of hydrazide-hydrazone derivatives and their evaluation of antidepressant, sedative and analgesic agents**,** Journal of Pharmaceutical Sciences and Research**,** 2 (4):185-196. https://t.ly/w1mAx.

Monsen, R. C., Trent, J. O. (2018). G-quadruplex virtual drug screening: A review, Biochimie, 152:134-148. https://doi.org/10.1016/j.biochi.2018.06.024.

Nair, R. S., Kuriakose, M., Somasundaram, V, *et al*. (2014). The molecular response of vanadium complexes of nicotinoyl hydrazone in cervical cancers--a possible interference with HPV oncogenic markers, Life Sciences, 116 (2):90-97. https://doi.org/ 10.1016/j.lfs.2014.09.011.

Ngoepe, M. P., Clayton, H. S. (2021). Metal Complexes as DNA Synthesis and/or Repair Inhibitors: Anticancer and Antimicrobial Agents, Pharmaceut Fronts, 3:e164-e182. https://doi.org/10.1055/s-0041-1741035.

Palma, E., Carvalho, J., Cruz, C., Paulo, A. (2021). Metal-Based G-Quadruplex Binders for Cancer Theranostics, Pharmaceuticals (Basel), 14 (7):605. https://doi.org/ 10.3390/ph14070605.

Popiołek, Ł. (2017). Hydrazide–hydrazones as potential antimicrobial agents: overview of the literature since 2010, Med Chem Res, 26:287-301. https://doi.org/10.1007/s00044-016-1756-y.

Prescott, B. (1975). Thiosemicarbazones and hydrazones of alpha-methylchalkone as potential chemotherapeutic agents, International Journal of Clinical Pharmacology and Biopharmacy. (4) :332-335. PMID: 1099024.

Rollas, S., Gulerman, N., Erdeniz, H. (2002). Synthesis and antimicrobial activity of some new hydrazones of 4-fluorobenzoic acid hydrazide and 3-acetyl-2,5-disubstituted-1,3,4-oxadiazolines, Farmaco, 57 (2):171-174. https://doi.org/10.1016/s0014-827x(01)01192-2.

Sastry, C. S. P., Rao, A. R. (1989). Spectrophotometric determination of some analgesic and anti-inflammatory agents with 3-methyl-2-benzothiazolinone hydrazone hydrochloride, Mikrochim Acta, 97:237-244. https://doi.org/10.1007/BF01242470.

Şenkardeş, S, Han Mİ, Kulabaş N, *et al.* (2020). Synthesis, molecular docking and evaluation of novel sulfonyl hydrazones as anticancer agents and COX-2 inhibitors. Molecular Diversity. 24 (3):673-689. https://doi.org 10.1007/s11030-019-09974-z.

Sharma, A., Kumar, V., Jain, S., Sharma, P. C. (2011). Thiazolidin-4-one and hydrazone derivatives of capric acid as possible anti-inflammatory, analgesic and hydrogen peroxide-scavenging agents, J Enzyme Inhib Med Chem, (4):546-52. https://doi: 10.3109/14756366.2010.535796.

Singh, K. D., Unal, H., Desnoyer, R., Karnik, S. S. (2018). Divergent Spatiotemporal Interaction of Angiotensin Receptor Blocking Drugs with Angiotensin Type 1 Receptor, J Chem Inf Model, 58 (1):182-193. https://doi.org/10.1021/acs.jcim.7b00424.

Sinha, R., Sara, U.V.S., Khosa, R.L., Stables, J., Jain, J. (2011). Nicotinic acid hydrazones: a novel anticonvulsant pharmacophore, Med Chem Res, 20:1499-1504. https://doi.org/10.1007/s00044-010-9396-0.

Suntharalingam, K., White, A. J. P., Vilar, R. (2009). Synthesis, Structural Characterization, and Quadruplex DNA Binding Studies of Platinum(II)-Terpyridine Complexes, Inorg. Chem, 48 (19):9427-9435. https://doi.org/10.1021/ic901319n.

Tian, J.,Ji, R.,Wang, H., Li, S., Zhang, G. (2022). Discovery of Novel α-Aminophosphonates with Hydrazone as Potential Antiviral Agents Combined with Active Fragment and Molecular Docking, Frontiers in chemistry, 10(ID:911453). https:doi.org/10.3389/fchem.2022.911453.

Verma, G., Marella, A., Shaquiquzzaman, M., Akhtar, M., Ali, M.R., Alam, M.M. (2014). A review exploring biological activities of hydrazones, J Pharm Bioallied Sci, 6 (2):69-80. https://doi: 10.4103/0975-7406.129170.

Wu, Y., Ding, X., Ding, L., Zhang, Y., Cui, L., Sun, L., Li, W., Wang, D., Zhao, Y. (2018). Synthesis and antibacterial activity evaluation of novel biaryloxazolidinone analogues containing a hydrazone moiety as promising antibacterial agents, Eur J Med Chem, 158:247-258. https://doi.org/10.1016/j.ejmech.2018.09.004.

Wang, P., Leung, C. H., Ma, D. L., Yan, S. C., Che, C. M. (2010). Structure-based design of platinum(II) complexes as c-myc oncogene down-regulators and luminescent probes for G-quadruplex DNA, Chemistry,16 (23):6900-6911. https://doi.org/10.1002/chem.201000167.

Submitted: 20/07/2022
Revised: 06/09/2022
Accepted: 08/09/2022
DOI: 10.48129/kjs.21599